Nanoscale

RSC Publishing

COMMUNICATION

Fuel concentration dependent movement of supramolecular catalytic nanomotors†

Cite this: *Nanoscale*, 2013, **5**, 1315

Received 28th September 2012
Accepted 21st November 2012

DOI: 10.1039/c2nr32976j

www.rsc.org/nanoscale

Daniela A. Wilson,*[a] Bart de Nijs,[b] Alfons van Blaaderen,[b] Roeland J. M. Nolte[a] and Jan C. M. van Hest*[a]

The effect of the fuel concentration on the movement of self-assembled nanomotors based on polymersomes is reported. Positive control over the speed of the nanomotors and insights into the mechanism of propulsion are presented.

The discovery of the operating mechanism of motor proteins and their assemblies has generated futuristic visions of building tiny cars, aircrafts, submarines as small as bacteria, and microscopic surgeons able to reach infected organs and cure diseases.[1–4] Much progress has been made at the molecular level from molecular rotors, ratchets, switches or shuttles using exceptional control over the chemistry and conformation of molecules under external stimuli.[5–11] Since the first self-propelled centimeter-sized platinum plates, capable of converting chemical energy into autonomous movement, were reported by Whitesides *et al.*,[12] many groups have focused on the design of artificial motors of smaller sizes by using a top-down approach.[13–24] Interesting examples have been reported using innovative engineering at the macroscale.[13–25] The motors were developed from either asymmetric bimetallic catalytic rods or spheres or symmetric rolled-up microtube jet engines obtained by photolithography techniques. The propulsion of the bimetallic rods in hydrogen peroxide was mainly driven by electrophoretic mechanisms[13,14] except in the presence of surfactants when bubble driven propulsion was observed.[13c] The movement of the microtube jet engines was driven by the accumulation of oxygen bubbles produced by the platinum catalyst within the inner wall. Although the positioning of the active catalyst is symmetrically distributed, the asymmetry resulted from the difference in the diameters of the opening in the conical shape making bubbles to migrate towards the larger tubular diameter.[16] The construction of artificial motor systems with all three dimensions in the nanometer range that have the capacity to move autonomously and perform diverse tasks is still a challenge to achieve with synthetic building blocks. We have recently shown that shape transformation of polymeric vesicles can lead to a new type of nanomotor by creating a folded structure with a cavity containing platinum nanoparticles. In the presence of hydrogen peroxide, which is converted to molecular oxygen and water by the active platinum centers, the nanomotor can move as demonstrated by nanoparticle tracking analysis (NTA).[27] Here we describe how the speed of these nanomotors can be controlled by varying the fuel concentration from which information about the mechanism of movement can be obtained. The speed of the nanomotors can be efficiently controlled even at very low concentrations of the fuel while the amount of fuel determines the prevalence of the two competing mechanisms: bubble propulsion or self-diffusiophoresis.

Polymer vesicles assembled from amphiphilic block copolymers can change their shape using osmotic shock to form kinetically trapped bowl shaped structures.[26–29] Strict control over the opening is obtained by controlling the flexibility of the polymersome membrane *via* the rate of solvent expulsion by dialysis.[27a] Nanometer bowl-shaped structures were reported with openings from hundreds of nanometers to completely closed structures.[27] The bowl shaped morphology was ideal for nanoparticle entrapment and we demonstrated that this can be achieved either during the supramolecular assembly and shape transformation into the folded morphology or by using the nanocavity of such structures to generate *in situ* nanoparticles.[30]

Previously, 2D TEM structural analysis was performed to demonstrate the entrapment of the catalytically active nanoparticles inside the structure, while nanoparticle-tracking analysis (NTA) was used to prove the movement of the nanomotor. However to provide absolute proof for the positioning of the active Pt nanoparticles inside the cavity we have now used 3D electron tomography, which allows for successive tilt acquisitions and 3D reconstruction of the nanomotor (Fig. 1, S1 and S2†).

[a]*Radboud University Nijmegen, Institute for Molecules and Materials, Heyendaalseweg 135, 6525 AJ, Nijmegen, The Netherlands. E-mail: d.wilson@science.ru.nl; Fax: +31 243653393; Tel: +31 243652381*

[b]*University of Utrecht, Debye Institute for NanoMaterials Science, Soft Condensed Matter, Princetonplein, 3508 TA, Utrecht, The Netherlands*

† Electronic supplementary information (ESI) available: Materials and instrumentation, formation of polymersomes and shape transformation, assembly of the nanomotors and details of the electron tomography of stomatocytes and self-assembled nanomotors. See DOI: 10.1039/c2nr32976j

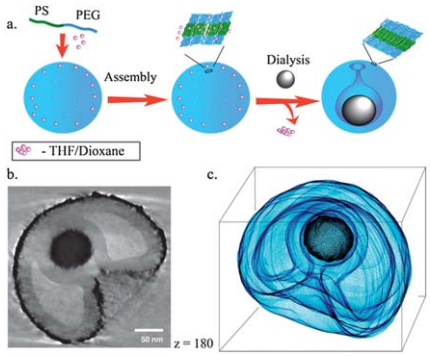

Fig. 1 Supramolecular assembly of the stomatocyte nanomotor: (a) schematic representation of the shape transformation and nanoparticle entrapment, (b) electron tomography image of a cross-section through the stomatocyte nanomotor and (c) 3D electron reconstruction of the nanoparticle filled stomatocyte.

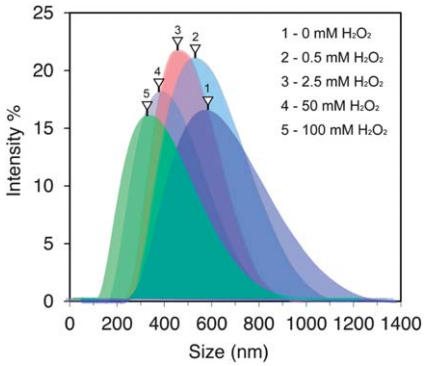

Fig. 2 Decrease in the size of the stomatocyte nanomotors after sequential addition of fuel by DLS (final fuel concentration).

Indeed the tomography profile reconstructed from the electron microscopy images of the stomatocytes showed clearly the inclusion of only one nanoparticle inside the structure, when platinum nanoparticles larger than 80 nm were used for the entrapment during the shape transformation. The platinum nanoparticles entrapped were highly branched and therefore displayed excellent performance in catalytic applications. They were obtained *via* a modified sonication technique reported by Yamauchi and Wang.[31] Such particles are known to decompose hydrogen peroxide into water and oxygen and the fast discharge of gases from the entrapped nanoparticles was shown to generate propulsive movement of the supramolecular structures.[29]

The propelling effect of the rapid discharge of gases during the catalytic decomposition of hydrogen peroxide was expected to be dependent on the concentration of the fuel. In our previous proof of concept study we used only one concentration to demonstrate the autonomous movement of the nanomotor and could not distinguish between different possible mechanisms of movement. A detailed analysis of the autonomous movement in the presence of varying concentrations of H_2O_2 was therefore carried out by using two techniques: Dynamic Light Scattering (DLS) and NTA. Dynamic light scattering is a technique frequently used for determination of the size of nanoparticles and nanostructures and applies for particles suspended in solution under random Brownian motion. However when propulsive directional movement replaces the Brownian motion during the catalytic reaction, the apparent diffusion coefficient increases due to faster movement. This results in a decrease in the apparent size of the nanomotors as the size and diffusion are inversely correlated through the Stokes–Einstein equation. A decrease was observed in the size of the motor proportional to the amount of fuel added to the nanomotors suggesting, as expected, that the particles increase their speed as more hydrogen peroxide is decomposed by the catalytic active nanoparticle (Fig. 2). This effect was not observed in the control experiments with empty stomatocytes lacking the active catalyst or non-encapsulated particles, which were treated with the same amount of hydrogen peroxide. Although dynamic light scattering was useful in demonstrating the autonomous movement of the nanomotors in a larger solution volume, it could not provide particle-by-particle analysis and insight into the movement mechanism of the nanomotors at different concentrations of the fuel. This information was only attainable *via* the nanoparticle tracking analysis technique, which allows individual particle-by-particle analysis from the determination of the tracking coordinates, particle trajectories and mean square displacements at different concentrations of fuel.[29,32]

Analysis of the mean square displacement of 110 nanomotors that ranged from 110 nm to 357 nm at different fuel concentrations illustrated an interesting effect. While small amounts of fuel (0.1–5 μl, 0.5–20 mM) indeed showed an increase in the mean square displacement (MSD) when compared to the control with a linear fit of the MSD, the higher concentrations (5–20 μl, 20–100 mM) of the fuel showed propulsive and directional movement of the motors with a parabolic fit of the MSD. This different behavior can be explained by the relative contribution of 2 propulsion mechanisms, namely bubble propulsion and self-diffusiophoresis (self-generated local concentration gradient of dissolved oxygen), which are expected to operate simultaneously.[24,25] We think that the relative contribution of these two mechanisms is dependent on the amount of fuel used during the experiment as suggested by the MSD curves (Fig. 3). At low fuel injections the amount of oxygen produced by the motors is probably low enough to be dissolved in the surrounding environment generating a local concentration gradient responsible for the self-diffusiophoresis mechanism in asymmetric structures like the stomatocyte nanomotor. As the concentration of the hydrogen peroxide increases, the rate of oxygen production is also expected to increase to the point where the full dissolution of the oxygen into the surrounding media is no longer possible. For this case we expect that the bubble propulsion mechanism would subdue the diffusion mechanism resulting in a parabolic fit of the MSD as demonstrated in Fig. 3. It is remarkable that even very small concentrations of fuel (0.005–0.05% v/v) can generate propulsive autonomous movement of the nanomotors with the lowest speed of 6.6 μm s^{-1}, while previous studies showed consistent loss in directionality and speed for concentrations smaller than 5% v/v.[13a,25] Furthermore, we were able to record the trajectories of the nanomotors and analyze their movement. Interestingly, from a total number of 97 trajectories recorded for the 15 μl fuel addition, 29 resembled the "tumble and run" features of bacterial movement. We believe that these small interruptions in the directional movement, at high concentrations of the fuel, could be due to the

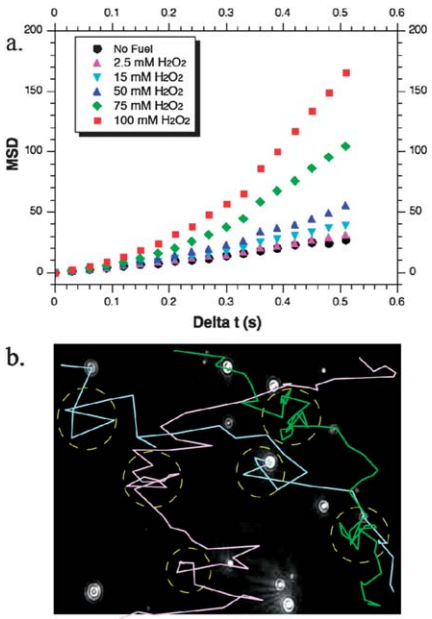

Fig. 3 (a) Average MSD of the platinum-loaded stomatocytes before and after the addition of different amounts of H_2O_2 (final fuel concentration) calculated from the tracking coordinates of 110 particles from the major size distribution. (b) Typical trajectories of the supramolecular nanomotor after 15 μl fuel addition.

intrinsic design of the motor that allows access of the fuel only by diffusion. When the rate of oxygen production is quite high, this can result in fast consumption of the "reservoir" and subsequent short time restoration of the Brownian movement until the next refill with "fresh" fuel is established. Self-assembly is therefore a powerful tool in the bottom-up design of supramolecular locomotive structures. Polymeric vesicles have already found many applications from the medical field, drug delivery to nanoreactors applications. Placing a motor inside such structures appends the locomotive abilities, which can overcome the slow undirected diffusion limitation of such delivery systems. Therefore understanding the influence of concentration and the mechanism of movement of such systems is crucial for future applications.

Conclusions

We have provided firm proof of the structure of platinum containing stomatocyte nanomotors, previously reported by us, by applying 3D electron tomography. Furthermore, NTA experiments revealed that the movement of the nanomotors is controlled by two mechanisms: self-diffusiophoresis and bubble propulsion, the first operating at low and even very low fuel concentrations. Interesting insights into the mechanism of movement at different fuel concentrations are discussed.

Acknowledgements

This work was supported by the European Research Council under the European Union's Seventh Framework Programme (FP7/2007-2012)/ERC-StG 307679 "StomaMotors" (D.A.W.). Financial support from the Dutch Science Foundation under the VICI-project Kinetically controlled peptide–polymer artificial organelles (J.C.M.vH) and ERC Advg 290886 "ALPROS" (R.J.M.N.) is kindly acknowledged.

Notes and references

1 J. A. Spudich, *Science*, 2011, **331**, 1143.
2 M. Schliwa and G. Woehlke, *Nature*, 2003, **422**, 759–765.
3 M. G. L. van den Heuvel and C. Dekker, *Science*, 2007, **317**, 333.
4 E. R. Kay, D. A. Leigh and F. Zerbetto, *Angew. Chem., Int. Ed.*, 2007, **46**, 72.
5 (*a*) N. Koumura, R. W. Zijlstra, R. A. van Delden, N. Harada and B. L. Feringa, *Nature*, 1999, **401**, 152; (*b*) J. R. A. van Delden, *et al.*, *Nature*, 2005, **437**, 1337.
6 T. R. Kelly, H. De Silva and R. A. Silva, *Nature*, 1999, **401**, 150–152.
7 D. A. Leigh, J. K. Y. Wong, F. Dehez and F. Zerbetto, *Nature*, 2003, **424**, 174.
8 J. D. Badjic, V. Balzani, A. Credi, S. Silvi and J. F. Stoddart, A molecular elevator, *Science*, 2004, **303**, 1845.
9 M. F. Hawthorne, J. I. Zink, J. M. Skelton, M. J. Bayer, C. Liu, E. Livshits, R. Baer and D. Neuhauser, *Science*, 2004, **303**, 1849.
10 (*a*) S. P. Fletcher, F. Dumur, M. M. Pollard and B. L. Feringa, *Science*, 2005, **310**, 80; (*b*) T. Kudernac, N. Ruangsupapichat, M. Parschau, B. Maciá, N. Katsonis, S. R. Harutyunyan, K.-H. Ernst and B. L. Feringa, *Nature*, 2011, **479**, 208.
11 C. Mao, W. Sun, Z. Shen and N. C. Seeman, *Nature*, 1999, **397**, 144.
12 R. Ismagilov, A. Schwartz, N. Bowden and G. M. Whitesides, *Angew. Chem., Int. Ed.*, 2002, **41**, 652.
13 (*a*) W. Paxton, K. Kistler, C. Olmeda, A. Sen, S. Angelo, Y. Cao, T. Mallouk, P. Lammert and V. Crespi, *J. Am. Chem. Soc.*, 2004, **126**, 13424; (*b*) T. Kline, W. Paxton and T. Mallouk, *Angew. Chem., Int. Ed.*, 2005, **117**, 754; (*c*) G. A. Ozin, I. Manners, S. Fournier-Bidoz and A. Arsenault, *Adv. Mater.*, 2005, **17**, 3011.
14 (*a*) U. Demirok, R. Laocharoensuk, K. M. Manesh and J. Wang, *Angew. Chem., Int. Ed.*, 2008, **120**, 9489; (*b*) W. Gao, S. Sattayasamitsahit, J. Orozco and J. Wang, *J. Am. Chem. Soc.*, 2011, **133**, 11862.
15 A. Solovev, Y. Mei, E. B. Urena, G. Huang and O. G. Schmidt, *Small*, 2009, **14**, 1688.
16 (*a*) Y. F. Mei, G. Huang, A. A. Solovev, E. B. Urena, I. Monch, F. Ding, T. Reindl, R. K. Y. Fu, P. K. Chu and O. G. Schmidt, *Adv. Mater.*, 2008, **20**, 4085; (*b*) S. Sanchez, A. Solovev, S. M. Harazim and O. G. Schmidt, *J. Am. Chem. Soc.*, 2011, **133**, 701; (*c*) Y. Mei, A. A. Solovev, S. Sanchez and O. G. Schmidt, *Chem. Soc. Rev.*, 2011, **40**, 2109; (*d*) A. A. Solovev, W. Xi, D. H. Gracias, S. M. Harazim, C. Deneke, S. Sanchez and O. G. Schmidt, *ACS Nano*, 2012, **6**, 1751.
17 (*a*) V. J. Eelkema, R. W. R. Browne, A. Meetsma, R. M. La Crois and B. L. Feringa, *Chem. Commun.*, 2005, 3936; (*b*) D. Pantarotto, W. R. Browne and B. L. Feringa, *Chem. Commun.*, 2008, 1533; (*c*) C. Stock, N. Heureux and

W. R. Browne, *et al.*, *Chem.–Eur. J.*, 2008, **14**, 3146; (*d*) N. Heureux, F. Lusitani and W. R. Browne, *et al.*, *Small*, 2008, **4**, 76–480.
18 J. Wu, S. Balasubramanian, D. Kagan, K. M. Manesh, S. Campuzano and J. Wang, *Nat. Commun.*, 2010, **1**, 1.
19 K. M. Manesh, *et al.*, *ACS Nano*, 2010, **4**, 1799.
20 S. Balasubramanian, D. Kagan, C.-M. J. Hu, S. Campuzano, M. J. L. Castanon, N. Lim, D. Y. Kang, M. Zimmerman, L. Zhang and J. Wang, *Angew. Chem., Int. Ed.*, 2011, **123**, 4247.
21 (*a*) M. Pumera, *Nanoscale*, 2010, **2**, 1643; (*b*) G. Zhao, T. H. Seah and M. Pumera, *Chem.–Eur. J.*, 2011, **17**, 12020; (*c*) G. Zhao, S. Sanchez, O. G. Schmidt and M. Pumera, *Chem. Commun.*, 2012, **48**, 10090.
22 (*a*) J. G. Gibbs and Y. P. Zhao, *Appl. Phys. Lett.*, 2009, **94**, 163104; (*b*) J. G. Gibbs, S. Kothari, D. Saintillan and Y.-P. Zhao, *Nano Lett.*, 2011, **11**, 2543.
23 L. F. Valadares, *et al.*, *Small*, 2010, **6**, 565.
24 J. R. Howse, R. A. L. Jones, A. J. Ryan, T. Gough, R. Vafabakhsh and R. Golestanian, *Phys. Rev. Lett.*, 2007, 048102.
25 S. J. Ebbens and J. R. Howse, *Langmuir*, 2011, **27**, 12293.
26 (*a*) B. M. Discher, Y. Y. Won, J. C. M. Lee, F. S. Bates, D. E. Discher and D. A. Hammer, *Science*, 1999, **284**, 1143; (*b*) D. E. Discher and A. Eisenberg, *Science*, 2002, **297**, 967; (*c*) S. F. M. van Dongen, H. P. M. De Hoog, R. J. R. W. Peters, M. Nallani, R. J. M. Nolte and J. C. M. Van Hest, *Chem. Rev.*, 2009, **109**, 6212; (*d*) B. M. Rosen, C. J. Wilson, D. A. Wilson, M. R. Imam, M. Peterca and V. Percec, *Chem. Rev.*, 2009, **109**, 6275; (*e*) A. Blanazs, S. P. Armes and A. Ryan, *Macromol. Rapid Commun.*, 2009, **30**, 267.
27 For the use of platinum encapsulated stomatocytes as motor systems, see: (*a*) D. A. Wilson, R. J. M. Nolte and J. C. M. van Hest, *Nat. Chem.*, 2012, **4**, 268–274; (*b*) J. Howse, *Nat. Chem.*, 2012, **4**, 247–248.
28 K. T. Kim, J. Zhu, S. A. Meeuwisssen, J. J. L. M. Cornelissen, D. J. Pochan, R. J. M. Nolte and J. C. M. van Hest, *J. Am. Chem. Soc.*, 2010, **132**, 12522.
29 S. A. Meeuwissen, K. T. Kim, Y. Chen, D. J. Pochan and J. C. M. van Hest, *Angew. Chem., Int. Ed.*, 2011, **50**, 1.
30 D. A. Wilson, R. J. M. Nolte and J. C. M. van Hest, *J. Am. Chem. Soc.*, 2012, **134**, 9894.
31 L. Wang and Y. Yamauchi, *J. Am. Chem. Soc.*, 2009, **131**, 9152.
32 V. Filipe, A. Hawe and W. Jiskoot, *Pharm. Res.*, 2010, **27**, 796.

